

Experimental observation of solitary waves in a new designed pendulum chain system

Changqing Zhu^{1,3}, Juanmian Lei², Yecun Wu^{1,3}, Nan Li¹,
Da Chen¹ and Qingfan Shi¹

¹ Experimental Center of Physics, Beijing Institute of Technology, Beijing 100081, People's Republic of China

² School of Aerospace Engineering, Beijing Institute of Technology, Beijing 100081, People's Republic of China

E-mail: leijm@bit.edu.cn and qfshi123@bit.edu.cn

Received 6 November 2014, revised 22 February 2015

Accepted for publication 26 March 2015


Published 23 April 2015



CrossMark

Abstract

A new coupled pendulum chain system is developed to vividly simulate the solitary solutions of the sine-Gordon (SG) equation. Transmission processes of three kinds of solitons (kink, anti-kink and breather) are systematically observed by using a high speed camera system. The solutions of the SG equation are derived through deducing the net external torque of the pendulums. The experimental data obtained are consistent with the theoretical calculation, which verifies that the system designed is an effective device to demonstrate the nonlinear behaviour of solitary waves in teaching and learning.

 Online supplementary data available from stacks.iop.org/EJP/36/045002/mmedia

Keywords: SG equation, solitary wave, kink and anti-kink, breather

1. Introduction

Soliton, as a stable localized nonlinear wave and a well-known abstract concept, is still covered by a mysterious veil for a majority of people though it is now firmly established after a gestation period of more than one hundred years [1–4]. In fact, a soliton is a self-reinforcing wave that maintains its shape while it travels at a constant velocity. In the other hand, a soliton arises as the solution of a widespread class of weakly nonlinear dispersive partial differential equations describing a physical system from a mathematical perspective [5]. Specifically, the sine-Gordon (SG) equation expressed by $\partial^2 u / \partial t^2 - \partial^2 u / \partial x^2 + \sin u = 0$ is

³ These authors contributed equally to this work and should be considered co-first authors.

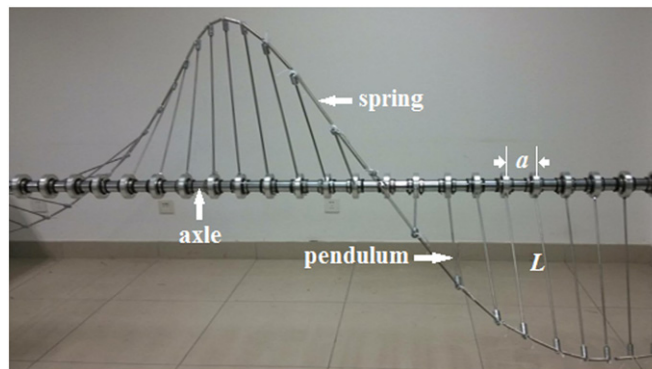


Figure 1. Photograph of the pendulum chain system.

a typical example of such equations in $(1+1)$ -dimensional space–time. Besides, the SG equation is associated with a completely integrable Hamiltonian system [6] and has three soliton solutions, i.e., kink, anti-kink and breather [7–9]. Furthermore, the soliton solutions are applied in many branches of physics, such as relativistic field theory [10], condensed matter physics [11], nonlinear optics [12], etc. Although there are many excellent textbooks at the introductory level [13–15] and a wealth of theoretical and numerical studies on the subject of solitons [4], it is still difficult to understand for undergraduate students. One of the key reasons is the scarcity of demonstration instruments for multifarious behaviours of solitary waves in nonlinear physics teaching.

In general, a solitary wave can be experimentally observed and extensively studied by an electrical or mechanical analogue. The electrical ones pick up nonlinear inductance and capacitance to numerically obtain soliton waveforms or pulse shaping in silicon [16, 17]. While the mechanical ones mainly focus on the kink and anti-kink soliton solutions. For instance, Dusuel *et al* construct a narrow kink in a strongly discrete chain of pendulums by which they model the dynamics of the compacton kinks and the kink-like modes [18]; Nakajima *et al* fabricate a system of aluminum discs to investigate the effect of loss and the effect of a distributed bias source [19]; Remoissenet manufactures a mechanical system in which the pendulums are elastically coupled by a torsional spring, and observes a breather soliton produced by a kink–antikink collision besides the collision of two kinks [4]. However, these experimental analogues are neither intuitive enough, nor detailed analysis for both torque of pendulums and derivation process of the SG equation. Therefore, it is necessary to develop a more precise and intuitive apparatus to demonstrate the propagation mechanism of solitary waves in physics study.

In this paper, we design a new mechanical analogue comprised of a pendulum chain coupled by the springs. The kink, anti-kink and breather solitons are observed by tracking the motion of each pendulum with a high-speed camera system. Based on the analysis of the external torque, the standardized SG equation is deduced and solved. The experimental results are in good agreement with the theoretical calculation. Teaching practice shows that the new coupled pendulum chain system is an effective, intuitive and reliable device for the student to view and understand the dynamic behaviours of solitons.

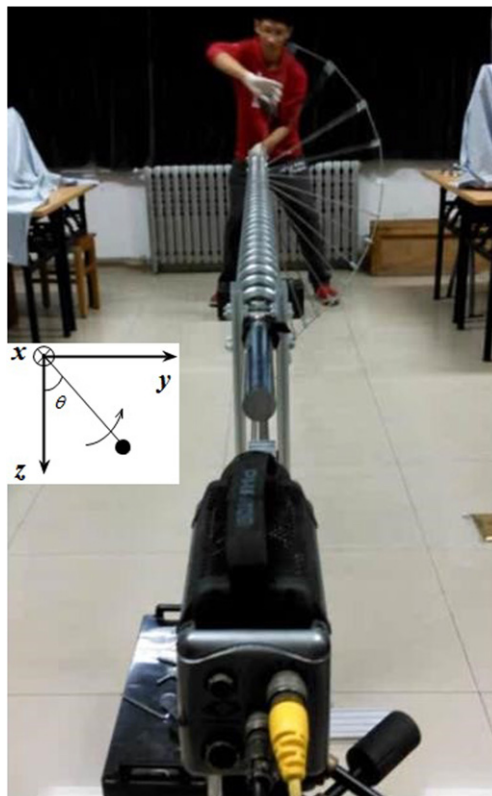


Figure 2. Sketch of an initial disturbance.

2. Experiments

2.1. Experimental set-up

The machinery system established is shown in figure 1, in which a chain of similar pendulums is mounted equidistantly along a horizontal axis, with adjacent pendulums being hinged with the springs end by end. Each pendulum can freely undergo an entire 360° revolution about the axle but cannot move sideways. Meanwhile, the movement of each pendulum can also drive the motion of its next one. When an initial disturbance is a complete rotation of the first pendulum, one can observe that this rotation result in a phase shift between the adjacent ones as shown in figure 2. Thus, a solitary wave propagates forward collectively along the transmission line, reflects at the opposite end, and travels again without any apparent modification of profile and velocity. For examining the properties of this localized wave, a high-speed camera system is used to observe the running track of each pendulum. A video demonstration of the results are given in the supplementary information, available at stacks.iop.org/EJP/36/045002/mmedia.

Here, we first describe the phase and the location of a pendulum by defining its angle θ relative to the plumb line and its location x relative to the i th pendulum at any time, respectively. The sign convention of θ is indicated in the inset of figure 2. Afterwards, we record the change of θ with time t and location x , so as to reveal whether the shape and

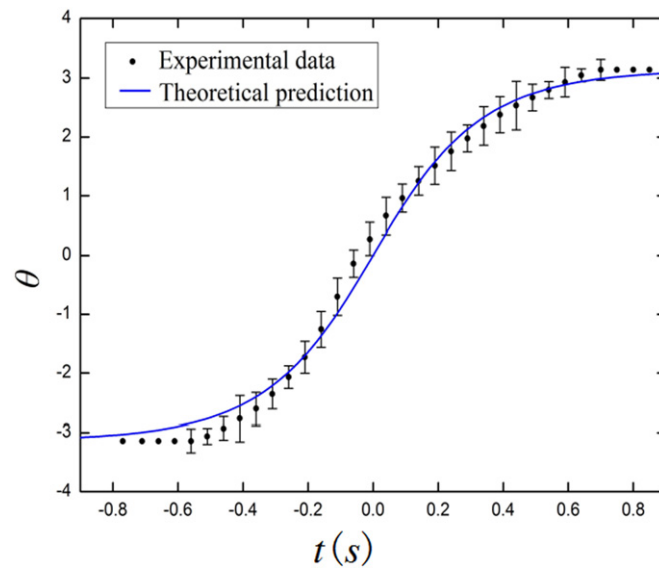


Figure 3. Swing angle θ versus time t .

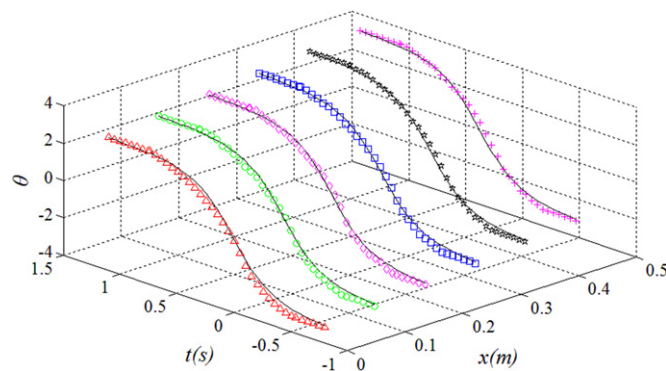


Figure 4. Swing angle θ varying with time t and location x . The different symbols stand for the six pendulums respectively.

velocity of solitary wave could be conserved. In experiment, the rotation of the chain is clockwise, and the starting position is its natural droop state. The swing angle θ of each pendulum is recorded once every 50 milliseconds.

2.2. Observation of kink and anti-kink

With the help of the camera, we first observe the dependence of the angle of rotation θ on time t for one pendulum in the chain. The experimental result is shown by the dots in figure 3, where minus θ means the swing angle of reversing rotation. After determining the motion property of a pendulum, we can investigate whether other pendulums move in the same way. Here, we may as well select six neighbouring pendulums.

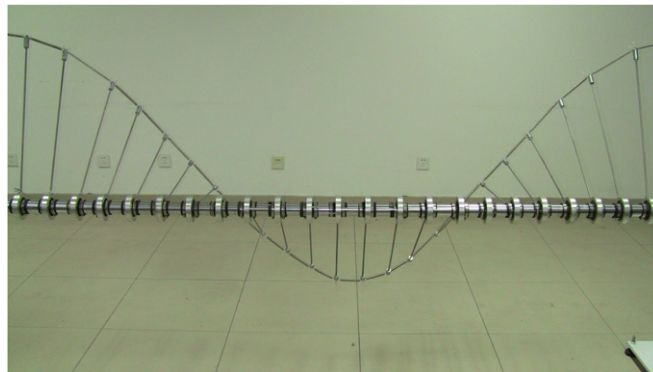


Figure 5. Photograph of a standing breather.

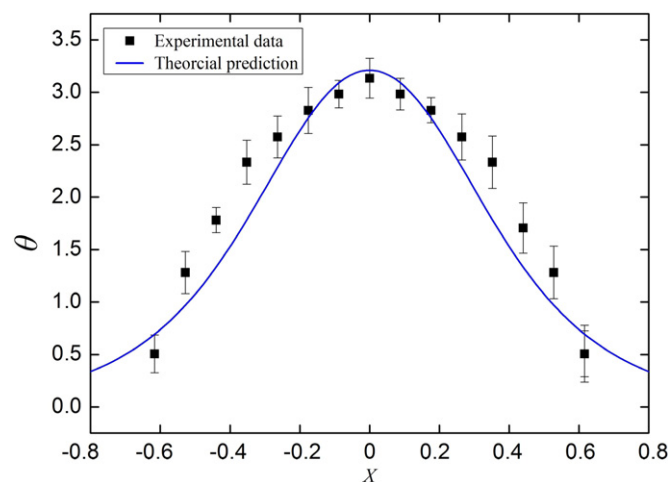


Figure 6. Representation of breather oscillation.

Figure 4 is the experimental result depicted in $(1+1)$ -dimensional space–time, where the different symbols stand for different pendulums. Apparently, the fluctuations of six pendulums have a time delay (lag effect) without an evident space dispersion (attenuation). So, all pendulums rotate regularly and successively one after another and follow the same propagation properties. In this case, a kink can be naturally observed. The kink, which is also called *topological soliton*, appears due to an inherent degeneracy of the system ground state. More specifically, a single kink can also be understood as a mathematical solution connecting two nearest identical minima of the periodic on-site potential. The other case of anti-kink is the same as the kink except their opposite direction. In summary, both the kink and the anti-kink can move freely along the chain without loss of energy for dissipation [18].

2.3. Experimental observation of breather

The so-called breather, whose name originates from the behaviour of its profile, repeats regularly oscillating upwards and downwards. It is a stationary-wave solution excited by a Hamiltonian in the centre of chain system as in the photograph shown in figure 5. The pulse

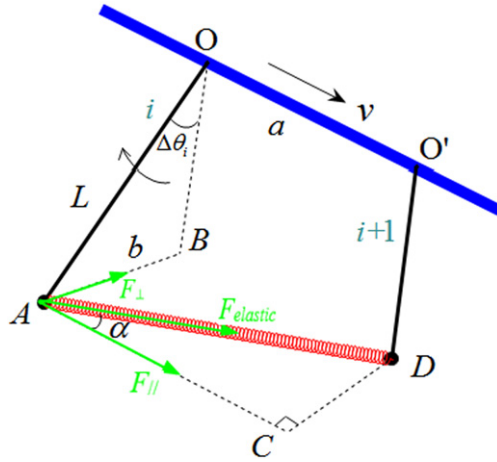


Figure 7. Force diagram for the neighbouring two pendulums rotating about the axle.

looks like breathing so that its relevant theory is called a breather mode, a breather soliton or a spatially localized oscillating nonlinear mode [18, 20]. In the experiment, the dependence of the angle of rotation θ on the location x of the pendulums is depicted in figure 6 in which X is a dimensionless quantity of x (see equation (18)).

3. Theoretical analysis

3.1. Deducing the net external torque

For the sake of clarity, we sketch the geometric diagram of the neighbouring i th and $(i+1)$ th pendulum in a moving moment as shown in figure 7. Here, L is the length of pendulum; a is the equidistant length along the axle as well as the initial length of the spring; α is the intersection angle between the spring and the horizontal axis. For facilitating the following analysis, some auxiliary lines are depicted in the figure, where AC is parallel to OO' , AB parallel to CD , OB parallel to $O'D$, and AC perpendicular to CD .

Let τ represent the net external torque acting upon the i th pendulum. τ is comprised of the elastic torque and the gravitational torque, i.e.

$$\tau = \tau_{\text{elastic}} + \tau_{\text{gravity}}, \quad (1)$$

where

$$\tau_{\text{elastic}} = \tau_{\text{elastic}}((i+1) \rightarrow i) - \tau_{\text{elastic}}((i-1) \rightarrow i), \quad (2)$$

and $\tau_{\text{elastic}}((i+1) \rightarrow i)$ means the elastic torque acting upon the i th pendulum by the $(i+1)$ th one, so dose $\tau_{\text{elastic}}((i-1) \rightarrow i)$.

To deduce τ_{elastic} , we first analyse the elastic force F_{elastic} acting upon a pendulum. We may as well use the symbol b to express the length of AB and easily obtain

$$b = 2L \sin\left(\frac{\Delta\theta_i}{2}\right), \quad (3)$$

where $\Delta\theta_i = \theta_i - \theta_{i+1}$ is the angle difference between the i th and $(i+1)$ th pendulum. Here θ_i is the i th pendulum's angle of rotation. Then the net elongation of the spring is

$$\Delta l = \sqrt{a^2 + b^2} - a. \quad (4)$$

According to Hooker's law $F_{\text{elastic}} = k\Delta l$, it can be rewritten as

$$F_{\text{elastic}} = k \left[\sqrt{a^2 + (2L \sin(\Delta\theta_i/2))^2} - a \right]. \quad (5)$$

where k is the stiffness coefficient of the spring.

Furthermore, we resolve F_{elastic} into its two components F_{\perp} and F_{\parallel} as shown in figure 7. Obviously

$$F_{\perp} = F_{\text{elastic}} \sin \alpha, \text{ and } F_{\parallel} = F_{\text{elastic}} \cos \alpha, \quad (6)$$

where

$$\alpha = \arcsin \left(\frac{b}{\sqrt{a^2 + b^2}} \right). \quad (7)$$

Actually, F_{\parallel} has no effect on the elastic torque and is negligible, so we have $\tau_{\text{elastic}}((i+1) \rightarrow i)$ by simultaneous equations (5), (6), and (7), i.e.

$$\begin{aligned} \tau_{\text{elastic}}((i+1) \rightarrow i) &= F_{\perp}(\Delta\theta_i)L \cos\left(\frac{\Delta\theta_i}{2}\right) = kL \left[\sqrt{a^2 + (2L \sin(\Delta\theta_i/2))^2} - a \right] \\ &\quad \cdot \frac{2 \sin(\Delta\theta_i/2)}{\sqrt{a^2 + (2L \sin(\Delta\theta_i/2))^2}} \cdot L \cdot \cos\left(\frac{\Delta\theta_i}{2}\right) \\ &= kL^2 \left[\sin(\Delta\theta_i) - \frac{\sin(\Delta\theta_i)}{\sqrt{1 + (2L \sin(\Delta\theta_i/2)/a)^2}} \right]. \end{aligned} \quad (8)$$

And similarly we can deduce that the elastic torque acting upon the i th pendulum by the $(i-1)$ th one is

$$\tau_{\text{elastic}}((i-1) \rightarrow i) = kL^2 \left[\sin(\Delta\theta_{i-1}) - \frac{\sin \Delta\theta_{i-1}}{\sqrt{1 + (2L \sin(\Delta\theta_{i-1}/2)/a)^2}} \right]. \quad (9)$$

Putting equations (8) and (9) into (2), we achieve the following equation

$$\tau_{\text{elastic}} = kL^2(\sin \Delta\theta_i - \sin \Delta\theta_{i-1} - c), \quad (10)$$

where

$$c = \frac{\sin(\Delta\theta_i)}{\sqrt{1 + (2L \sin(\Delta\theta_i/2)/a)^2}} - \frac{\sin(\Delta\theta_{i-1})}{\sqrt{1 + (2L \sin(\Delta\theta_{i-1}/2)/a)^2}}. \quad (11)$$

Owing to the case of $L \gg a$ and the relatively large elastic coefficient of the spring ($k = 195 \text{ N m}^{-1}$), $\Delta\theta_i$ should be small and $\sin \Delta\theta_i \sim \Delta\theta_i$. Accordingly, any term in equation (11) is a higher-order infinitesimal relative to $\sin \Delta\theta_i$ or $\sin \Delta\theta_{i-1}$. Thus we can omit c and equation (10) can be simplified to

$$\tau_{\text{elastic}} = kL^2(2\theta_i - \theta_{i-1} - \theta_{i+1}). \quad (12)$$

Due to the angle θ_i related to the position x , we can perform a Taylor expansion for the denominator of $\theta_{i\pm 1}$ to high order as the following

$$\theta_{i\pm 1} = \theta \pm a \frac{\partial \theta}{\partial x} + \frac{a^2}{2} \frac{\partial^2 \theta}{\partial x^2} \pm \frac{a^3}{3!} \frac{\partial^3 \theta}{\partial x^3} + \dots \quad (13)$$

Substituting equation (13) into (12), the elastic torque can be expressed by

$$\tau_{\text{elastic}} = -kL^2 a^2 \frac{\partial^2 \theta}{\partial x^2}. \quad (14)$$

Compared to the derivation process of elastic torque τ_{elastic} , the gravitational torque can be easily obtained as follows

$$\tau_{\text{gravity}} = mgL_c \sin \theta, \quad (15)$$

where mg is the gravity of one single pendulum, and L_c is the distance from its mass centre to the axle.

Finally, combining equations (1), (14) and (15), the net external torque is deduced as

$$\tau = mgL_c \sin \theta - kL^2 a^2 \frac{\partial^2 \theta}{\partial x^2}. \quad (16)$$

Based on the expression of τ , we can further deduce the standardized SG equation so as to reveal the propagation mechanism of solitary waves.

3.2. Deducing the standardized SG equation

Newton's second law for rotation is used to analyse the motion of a single pendulum, and we have

$$\tau = -I \frac{\partial^2 \theta}{\partial t^2}, \quad (17)$$

where I is the moment of inertia. Substitute equation (16) into (17), and transform the result into the dimensionless form. Eventually, we achieve the standardized form of SG equation

$$\frac{\partial^2 \theta}{\partial T^2} - \frac{\partial^2 \theta}{\partial X^2} + \sin \theta = 0, \quad \text{where } T = \sqrt{\frac{mgL_c}{I}} t, \quad \text{and } X = \sqrt{\frac{mgL_c}{a^2 k L^2}} x. \quad (18)$$

Equation (18) can be solved by inverse spectral transform method [21]. Its *kink* solution can be obtained as

$$\theta = -\pi + 4 \arctan \exp \left[\sigma (X - vT) / \sqrt{1 - v^2} \right] + \phi, \quad (19)$$

where $\sigma = \pm 1$ stands for the kink's so-called *topological charge*, ϕ is a constant, and v is the kink's velocity that cannot exceed its maximum value v_{max} (the sound velocity) [18]. The signs \pm of σ represent clockwise and anticlockwise rotation corresponding to a *kink* and an *anti-kink*, respectively. Based on equation (19), the calculated results for the change of swing angle with time and location are shown by the solid lines in figures 3 and 4.

Another solution of the SG equation is the *breather* as [4]

$$\theta = 4 \arctan \left[\frac{\sqrt{1 - \omega^2} \cos(\omega t)}{\omega} \operatorname{sech} \left(\sqrt{1 - \omega^2} x \right) \sin(\omega t) \right], \quad (20)$$

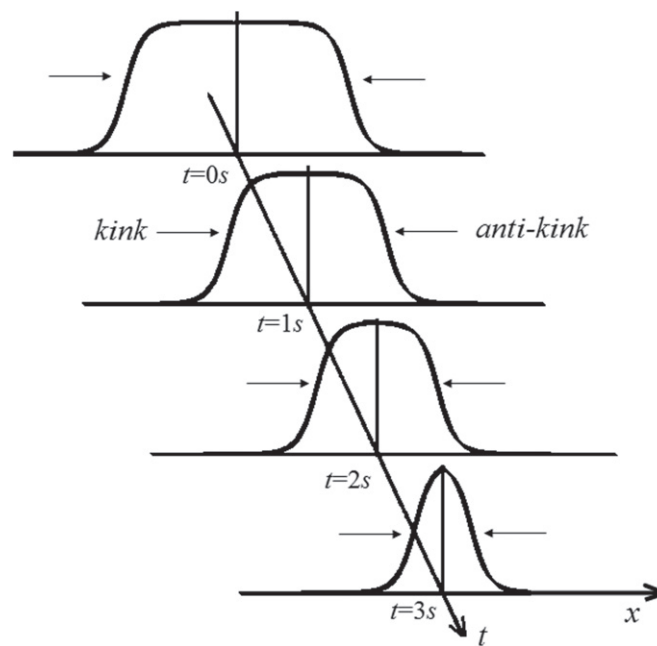


Figure 8. Bion's evolution with time sequency.

which describes a nonlinear state with internal frequency ω . Based on equation (20), the calculated result for the change of swing angle with location is shown by the solid line in figure 6. In the limit of low frequencies, $\omega \ll 1$, the breather can be qualitatively treated as a weakly coupled pair of kink and anti-kink [18]. In other words, the breather solution is equal to the collision of a kink and an anti-kink solution by combining equations (19) and (20). Hence it is also called a *bion*, and the numerical simulation for its evolution with time sequency is shown in figure 8.

4. Conclusions

A mechanical analogue of the SG equation is experimentally and theoretically investigated. Three solutions of the SG equation are calculated by analysing the elastic torque and gravitational torque of pendulums; various behaviours of solitary waves on a Josephson line are demonstrated on the mechanical transmission line. In conclusion, the newly designed pendulum chain system can be accepted as a structural basis for viewing and understanding the dynamic behaviours of complex nonlinear systems.

Acknowledgments

This work is supported by National Training Programs of Innovation and Entrepreneurship for Undergraduates of Beijing Institute of Technology (grant no. 201410007063), and the National Natural Science Foundation of China (grant no. 10975014).

References

- [1] Tang D Y, Zhang H, Zhao L M and Wu X 2008 Observation of high-order polarization-locked vector solitons in a fiber laser *Phys. Rev. Lett.* **101** 153904
- [2] Gardner C S, Greene J M, Kruskal M D and Miura R M 1967 Method for solving the Korteweg–deVries equation *Phys. Rev. Lett.* **19** 1095–7
- [3] Maxworthy T 1976 Experiments on collisions between solitary waves *J. Fluid Mech.* **76** 177–86
- [4] Remoissenet M 1999 *Waves Called Solitons: Concepts and Experiments* (Berlin: Springer) pp 137–58
- [5] Wikipedia 2014 Soliton (<http://en.wikipedia.org/wiki/Soliton>)
- [6] Ludwig D F and Leon T 1987 *Hamiltonian Methods in the Theory of Solitons* (reprint of 1st edn) (Berlin: Springer)
- [7] Kourakis I, Sultana S and Hellberg M A 2012 Dynamical characteristics of solitary waves, shocks and envelope modes in kappa-distributed non-thermal plasmas: an overview *Plasma Phys. Control. Fusion* **54** 124001
- [8] Bryden H L and Kinder T H 1991 Recent progress in strait dynamics *Rev. Geophys.* **29** 617–31
- [9] Salerno M 1991 *Phys. Rev. A* **44** 5292
- [10] Lennholm E and Hörnquist M 2003 Revisiting Salerno’s sine-Gordon model of DNA: active regions and robustness *Physica D* **177** 233–41
- [11] Bishop A R 1979 Solitons in condensed matter physics *Phys. Scr.* **20** 409–23
- [12] Mollenauer L F and Gordon J P 2006 *Solitons in Optical Fibers: Fundamentals and Applications* (California: Elsevier)
- [13] Gilbert R W, Zedler E A, Grilli S T and Street R L 2007 Progress on nonlinear-wave-forced sediment transport simulation *IEEE J. Ocean. Eng.* **32** 236–48
- [14] Drazin P G and Robin S J 1989 *Solitons: An introduction* (Cambridge: Cambridge University Press)
- [15] Wadati M 2001 Introduction to solitons *Pramana J. Phys.* **57** 841–7
- [16] Martín F and Oriols X 2001 Simple model to study soliton wave propagation in periodic-loaded nonlinear transmission lines *Appl. Phys. Lett.* **78** 2802–4
- [17] Afshari E and Hajimiri A 2005 Nonlinear transmission lines for pulse shaping in silicon *IEEE J. Solid-State Circuits* **40** 744–52
- [18] Braun O M and Kivshar Y S 2004 *The Frenkel–Kontorova Model: Concepts, Methods, Applications* (Berlin: Springer) pp 20–31
- [19] Nakajima K, Yamashita T and Onodera Y 1974 Mechanical analogue of active Josephson transmission line *J. Appl. Phys.* **45** 3141–5
- [20] Dauxois T, Peyrard M and Willis C R 1992 Localized breather-like solution in a discrete Klein–Gordon model and application to DNA *Physica D* **57** 267–82
- [21] Aktosun T 2009 Inverse scattering transform and the theory of solitons *Encyclopedia of Complexity and Systems Science* ed R A Meyers (New York: Springer) pp 4960–71